Compensation of Optical Nonlinear Waveform Distortion Using DSP-Based Reservoir Computing with Tapped Delay Lines

Kai Ikuta
School of Science and Technology
Meiji Univ.
Kawasaki, Kanagawa, Japan
k_ikuta@meiji.ac.jp

Yuta Ito
School of Science and Technology
Meiji Univ.
Kawasaki, Kanagawa, Japan
ee191143@meiji.ac.jp

Moriya Nakamura
School of Science and Technology
Meiji Univ.
Kawasaki, Kanagawa, Japan
m_naka@meiji.ac.jp

***Abstract*— We propose a novel reservoir-computing-based nonlinear equalizer, designed to compensate for fiber-optic nonlinearity. Signals are fed to the equalizer through tapped delay lines. We clarified that the equalizer outperforms conventional alternatives.**

Keywords*— *Reservoir computing, Nonlinear equalization, Optical nonlinearity, Coherent detection

I. INTRODUCTION

Digital coherent technology improves the receiver sensitivity and spectral efficiency of optical communication systems, while also enabling compensation of waveform distortion using digital signal processing (DSP). Compensation for linear waveform distortion caused by, e.g., chromatic dispersion and polarization mode dispersion (PMD) has already been implemented in practical systems. DSP can also be utilized to compensate for nonlinear distortion caused by optical nonlinear effects such as self-phase modulation (SPM) and cross-phase modulation (XPM). Some nonlinear equalization algorithms have been investigated, including digital backpropagation (DBP) and Volterra series transfer function (VSTF) [1-3]. However, DBP and VSTF require significant computational resources, which increase the signal delay and the power consumption at the DSP. The nonlinear equalization algorithm based on artificial neural networks (ANNs) is gaining attention due to its ability to significantly reduce the computational complexity [4-8]. One proposal achieved polarization tracking and the nonlinear equalization at the same time [9,10]. In these studies, ANNs of multilayer type have been employed. To train the multilayer ANNs, error backpropagation (EBP) algorithm is used, which updates the weights and biases of the ANN units while propagating the error from the output layer to the input layer. However, this algorithm requires more computational complexity compared to training algorithms used for finite impulse response (FIR) filters, such as the standard least mean square (LMS) algorithm. Therefore, it poses a challenge for applications that require continuous high-speed learning, such as polarization tracking. On the other hand, nonlinear equalizers based on reservoir computing (RC) are also being investigated [11]. The RC includes a reservoir layer which consists of a recurrent-ANN (RNN) with randomly preset and fixed weights. Only output-layer weights are trained using the LMS algorithm, allowing the equalizer to compensate for the nonlinear waveform distortion. This approach enables fast training comparable to that of FIR filters. The proposed implementation methods include utilizing optical nonlinear effects of optical devices such as optical fibers and semiconductor optical amplifiers (SOA) to achieve the reservoir-layer function [12, 13] and employing DSP to perform the RC operations [14]. The RC has the property of storing input signals in the reservoir, which makes it possible to compensate for distorted time-spread signals using the stored signals. The length of the stored signal is determined by the length of the RC's impulse response. In some cases, however, it can be difficult to obtain the impulse response of sufficient length [13]. Additionally, even if the impulse response is long enough, the quality of the stored signals deteriorates over time, which will result in a degradation of the compensation performance. In this paper, we propose a novel RC-based nonlinear equalizer in which signals are fed through tapped delay lines. We evaluated the performance of the nonlinear equalization using numerical simulations.

II. RC-BASED NONLINEAR EQUALIZER AND IMPULSE RESPONSE

Fig. 1 schematically shows the construction of the commonly used RC-based nonlinear equalizer, which consists of input layer, reservoir layer, and output layer. The reservoir is composed of an RNN. The weights of the input and reservoir layers are preset randomly and remain fixed. Only the weights of the output layer are trained using the LMS algorithm. The input and output layers each have two units to accommodate the in-phase (I) and quadrature (Q) components of the signals. The output of the reservoir units, $\boldsymbol{h}$, is described as [11]

$$\boldsymbol{h}(n) = f\left(\boldsymbol{w^{in}}\boldsymbol{x}(n) + \boldsymbol{w^{res}}\boldsymbol{h}(n-1)\right), \tag{1}$$

where $f(\cdot)$ is the activation function $f(u) = \tanh(u)$, $\boldsymbol{w^{in}}$ is the weight between the input-layer units and the reservoir units, $\boldsymbol{w^{res}}$ is the weight between the units in the reservoir, and $\boldsymbol{x}$ is the input to the input-layer units. The output of the output-layer units, $\boldsymbol{y}$, is described as

$$\boldsymbol{y}(n) = \boldsymbol{w^{out}}\boldsymbol{h}(n), \tag{2}$$

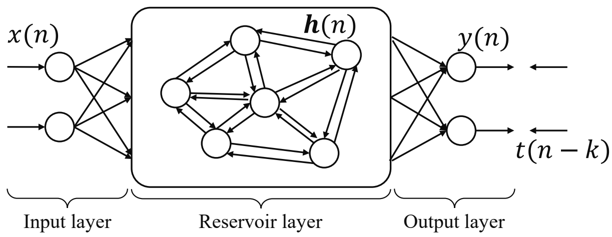

Fig.1. Conventional RC-based nonlinear equalizer.

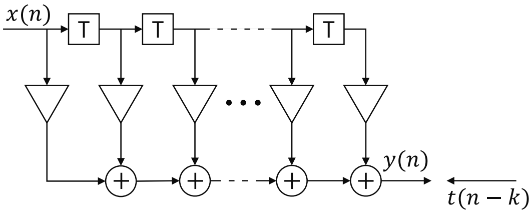

Fig. 2. FIR filter.

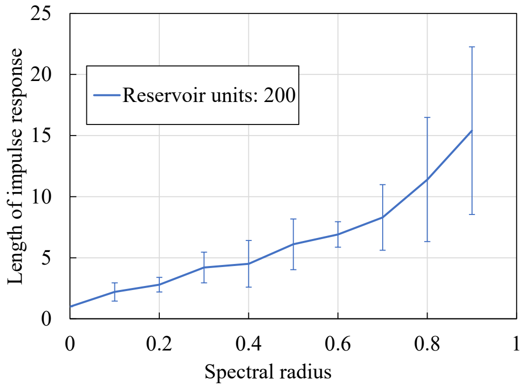

Fig. 3. Length of impulse response versus spectral radius.

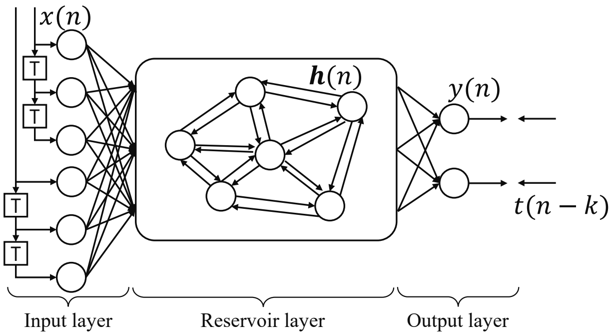

Fig. 4. Proposed RC-based nonlinear equalizer with tapped-delay lines.

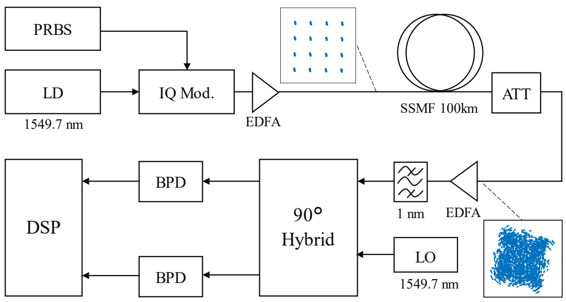

Fig. 5. System setup of 16QAM optical-fiber transmission.

where $\boldsymbol{w}^{out}$ is the weight between the reservoir units and output-layer units. In the learning process of the RC, only the weight, $\boldsymbol{w}^{out}$, is updated using the LMS algorithm to minimize the error, e, which is expressed as

$$e = \frac{1}{2}\left(\boldsymbol{y}(n) - \boldsymbol{t}(n-k)\right)^2, \tag{3}$$

where $\boldsymbol{t}$ represents the supervisory signal, k is the time shift between the received signal (input to the input-layer units) and the supervisory signal. The value of k is a parameter that affects the performance of the equalizer. The meaning of the parameter, k, can be understood through an analogy with a conventional FIR filter shown in Fig. 2. When using an FIR filter to compensate for chromatic dispersion in an optical fiber, the time shift, k, is typically set to half the length of the tapped-delay line. The length of the tapped-delay line determines the length of impulse response of the FIR filter. Here, we consider the length of the impulse response of the RC-based nonlinear equalizer. The weights $\boldsymbol{w}^{in}$, and $\boldsymbol{w}^{res}$ of the RC are randomly preset and fixed as written above. However, $\boldsymbol{w}^{res}$ is scaled to satisfy the echo state property, which prevents oscillation of the RC and determines the length of the impulse response [11]. The condition is described as

$$\max(|\boldsymbol{\lambda}^{res}|) < 1, \tag{4}$$

where $\boldsymbol{\lambda}^{res}$ is the eigenvalue of the weight matrix, $\boldsymbol{w}^{res}$, and the left side of (4) is called a spectral radius, which determines the time constant and the impulse response of the RC [14]. Fig. 3 shows the length of the impulse response of the RC versus the spectral radius. Here, we defined the length of the impulse response as the number of response pulses until an impulse with a magnitude of 1 was applied to the RC, and its output attenuated to 1/100 (-20 dB). We plotted the averages of 10 trials in each condition, varying the weights randomly. The error bars represent the standard deviation. A larger spectral radius increases the length of the impulse response, and the signals to the RC are stored in the reservoir for an extended period. This result is consistent with the previous report [14]. However, when the spectral radius is large, the standard deviation of the impulse-response length also increases. This result indicates that it is difficult to achieve the RC with a long and stable impulse response. Additionally, even if the impulse response is long and stable, the quality of the stored signals deteriorates over time in the reservoir, which causes a degradation of the performance of the equalizer. Therefore, it is preferable to design the RC-based nonlinear equalizer with a small spectral radius. Fig. 4 shows our proposed RC-based nonlinear equalizer with feedforward tapped-delay lines. The IQ input signals are fed through the tapped-delay lines. We can realize the desired impulse-response length by adjusting the length of the tapped-delay lines. Furthermore, we can prevent the signal degradation in the reservoir, because we can employ the reservoir with a shorter impulse response. In this study, we employed the tapped-delay lines with a length of 3. The number of the reservoir units was 200. We did not utilize sparse connections for the reservoir units.

III. System Setup

Fig. 5 shows the 16QAM optical-fiber transmission system utilized in our numerical simulations. A 10-Gsymbol/s 16QAM optical signal was modulated by PRBS2^{15}-1 data and transmitted through a 100-km standard single-mode fiber (SSMF). The input signal power to the SSMF was as large as 12.5 dBm to induce the fiber nonlinearity. The optical signal was received using optical homodyne detection, with the assumption that the local oscillator (LO) was ideally phase-locked. The distorted signals after the transmission were compensated using the RC-based nonlinear equalizers in the DSP. The signal quality after the compensation was evaluated using error vector magnitude (EVM). The RC was also tested on some other data sets different from PRBS2^{15}-1 to ensure that no overfitting occurred after the learning process.

IV. Result and Discussion

Fig. 6(a) shows the EVM characteristics versus the spectral radius when we performed the nonlinear compensation using the conventional RC-based nonlinear equalizer without the tapped-delay lines. When the spectral

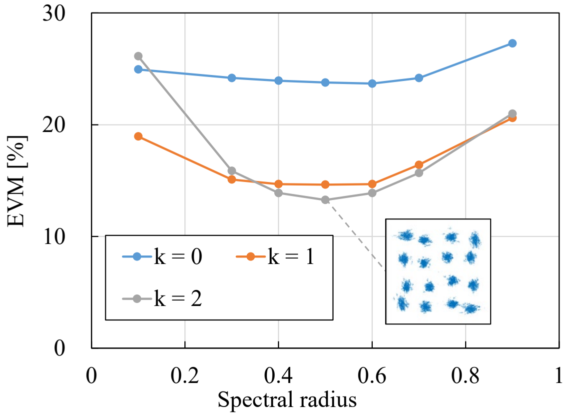

(a) w/o tapped-delay lines.

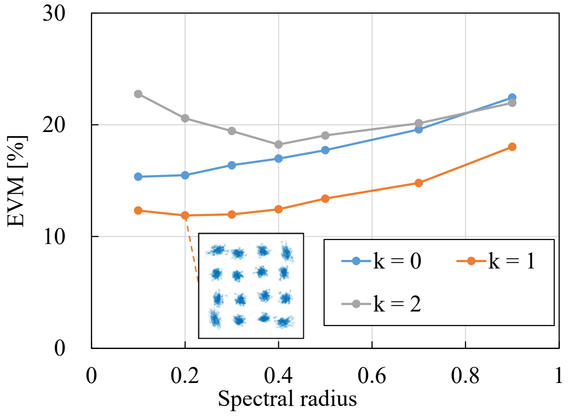

(b) w/ tapped-delay lines.

Fig. 6. EVM versus spectral radius.

radius was as small as 0.1, the equalizer could not achieve small EVMs. This is because, as shown in Fig. 3, the impulse response was not long enough, and the equalizer did not store sufficient signals for the compensation. When the spectral radius was increased to more than 0.6, the equalizer also failed to achieve low EVMs. This is because the impulse response was too long, and the retention of unnecessary signals in the reservoir degraded the compensation performance. The optimal EVM of 13.3% was achieved with the spectral radius of about 0.5. In this case, the impulse response was about 6 as shown in Fig. 3. The optimal time-shift, k, was 2. Fig. 6(b) shows the EVM characteristics versus the spectral radius when we performed the compensation using our proposed RC-based nonlinear equalizer with the tapped-delay lines. When the spectral radius was larger than 0.4, the equalizer could not achieve low EVMs due to the retention of the unnecessary signals in the reservoir. In this case, since the equalizer has the tapped-delay lines, the reservoir does not need to store long signals. The optimal EVM was achieved with the spectral radius of 0.2. The optimal time-shift was k=2. The achieved EVM was 11.9%, which was a 1.3% improvement compared to the case without the tapped-delay lines. The constellations at the optimal points are shown in the insets of Figs. 6(a) and (b). By using the tapped-delay lines, there is no need to employ the RC with a long time-constant, and the compensation performance is improved. However, the number of connections between the input-layer units and the reservoir units increases, which degrades the computational complexity of the equalizer. Nevertheless, since there is no change in the output layer, we can still take advantage of the fast learning characteristics of the RC-based nonlinear equalizer.

V. Conclusion

We proposed a novel RC-based nonlinear equalizer in which signals are input through the tapped-delay lines. The performance evaluation of nonlinear compensation revealed that the equalizer with tapped-delay lines outperformed conventional one.

Acknowledgment

This work was supported by JSPS KAKENHI Grant Number 20K05367.

References

[1] E. Ip and J. M. Kahn, "Compensation of dispersion and nonlinear impairments using digital backpropagation," *J. Lightw. Technol.*, vol. 26, no. 20, pp. 3416-3425, Oct. 2008.

[2] Y. Gao, F. Zhang, L. Dou, Z. Chen, and A. Xu, "Intra-channel nonlinearities mitigation in pseudo-linear coherent QPSK transmission systems via nonlinear electrical equalizer," *Optics Commun.*, vol. 282, no. 12, pp. 2421-2425, Jun. 2009.

[3] L. Liu, L. Li, Y. Huang, K. Cui, Q. Xiong, F. N. Hauske, C. Xie, and Y. Cai, "Intrachannel nonlinearity compensation by inverse Volterra series transfer function," *J. Lightw. Technol.*, vol. 30, no. 3, pp. 310-316, Feb. 2012.

[4] M. A. Jarajreh, E. Giacoumidis, I. Aldaya, S. T. Le, A. Tsokanos, Z. Ghassemlooy, and N. J. Doran, "Artificial neural network nonlinear equalizer for coherent optical OFDM," *IEEE Photon. Technol. Lett.*, vol. 27, no. 4, pp. 387-390, Feb. 2015.

[5] J. Estarán, R. Rios-Müller, M. A. Mestre, F. Jorge, H. Mardoyan, A. Konczykowska, J.-Y. Dupuy, and S. Bigo, "Artificial neural networks for linear and non-liner impairment mitigation in high-baudrate IM/DD systems," ECOC2016, M.2.B.2, Sep. 2016.

[6] S. Owaki, Y. Fukumoto, T. Sakamoto, N. Yamamoto, and M. Nakamura, "Experimental demonstration of SPM compensation based on digital signal processing using a three-layer neural-network for 40-Gbit/s optical 16QAM signal," *IEICE Commun. Express.*, vol. 7, no. 1, pp. 13-18, Jan. 2018.

[7] S. Owaki and M. Nakamura, "XPM compensation in optical fiber transmission systems using neural-network-based digital signal processing," *IEICE Commun. Express*, vol. 7, no. 1, pp. 31-36, Jan. 2018.

[8] M. Nakamura, Y. Fukumoto, S. Owaki, T. Sakamoto, and N. Yamamoto, "Experimental demonstration of SPM compensation using a complex-valued neural network for 40-Gbit/s optical 16QAM signals," *IEICE Commun. Express*, vol. 8, no. 8, pp. 281-286, Aug. 2019.

[9] Y. Kurokawa, T. Kyono, Y. Fukumoto, N. Sumimoto, and M. Nakamura, "Polarization demultiplexing and optical nonlinearity compensation based on artificial neural networks," *IEICE Commun. Express*, vol. 8, no. 12, pp. 542-547, Dec. 2019.

[10] Y. Kurokawa, T. Kyono, and M. Nakamura, "Polarization tracking and optical nonlinearity compensation using artificial neural networks," OECC2020, VP58, Oct. 2020.

[11] H. Jaeger, "The "echo state" approach to analysing and training recurrent neural networks," *Technical Report 148*, German National Research Center for Information Technology, Dec. 2001.

[12] M. Sorokina, S. Sergeyev, and S. Turitsyn, "Fiber echo state network analogue for high-bandwidth dual-quadrature signal processing," *Opt. Express*, vol. 27, no. 3, pp. 2387-2395, Feb. 2019.

[13] T. Tsurugaya, T. Hiraki, T. Aihara, M. Nakajima, N. P. Diamantopoulos, K. Takeda, T. Segawa, and S. Matsuo, "XPM-based reservoir computing using membrane MZM integrated with SOAs on Si," OECC2022, MD1-2, Jul. 2022.

[14] F. D. Ros, S. M. Ranzini, H. Bülow, and D. Zibar, "Reservoir-computing based equalization with optical pre-processing for short-reach optical transmission," *IEEE J. Sel. Top. Quantum Electron*, vol. 26, no. 5, Art no. 7701912, Sep./Oct. 2020.